Chemistry & Biology
Article

Structure-Activity Relationships of Antibacterial Acyl-Lysine Oligomers

Inna S. Radzishevsky,[1] Tchelet Kovachi,[1] Yaara Porat,[1] Lior Ziserman,[1] Fadia Zaknoon,[1] Dganit Danino,[1] and Amram Mor[1,*]
[1]Department of Biotechnology & Food Engineering, Technion-Israel Institute of Technology, Haifa 32000, Israel
*Correspondence: amor@tx.technion.ac.il
DOI 10.1016/j.chembiol.2008.03.006

SUMMARY

We describe structure-activity relationships that emerged from biophysical data obtained with a library of antimicrobial peptide mimetics composed of 103 oligoacyllysines (OAKs) designed to pin down the importance of hydrophobicity (H) and charge (Q). Based on results obtained with OAKs displaying minimal inhibitory concentration $\leq$ 3 μM, the data indicate that potent inhibitory activity of the gram-negative *Escherichia coli* and the gram-positive *Staphylococcus aureus* required a relatively narrow yet distinct window of HQ values where the acyl length played multiple and critical roles, both in molecular organization and in selective activity. Thus, incorporation of long—but not short—acyl chains within a peptide backbone is shown to lead to rigid supramolecular organization responsible for poor antibacterial activity and enhanced hemolytic activity. However, sequence manipulations, including introduction of a tandem lysine motif into the oligomer backbone, enabled disassembly of aggregated OAKs and subsequently revealed tiny, nonhemolytic, yet potent antibacterial derivatives.

INTRODUCTION

The success of infectious disease chemotherapy has been dimmed ever since the dawn of the antimicrobial drug era because of antibiotic resistance (Weber and Courvalin, 2005; MacKenzie et al., 2005). Today, because of the emergence of resistant organisms (Roos, 2004; Cookson, 2005), numerous diseases are becoming increasingly difficult to treat, including microorganisms responsible for severe infections in hospitalized patients, food-borne pathogens, and sexually transmitted pathogens, some of which are now resistant to most available antimicrobial drugs (Paterson, 2006; Rice, 2006; White et al., 2002). The clinical impact of resistance is immense, characterized by increased cost, morbidity, and mortality (Cassell, 1997; Howard et al., 2003), hence the importance of developing new antimicrobial agents (Bush, 2004). Due to exhausting efforts in the past 2 decades, low molecular weight peptide-based compounds, termed host defense peptides (HDPs) are increasingly recognized as a potential source for new antimicrobial agents (Zasloff, 2002; Jenssen et al., 2006). HDPs are products of evolutionary development, and their sequences and activities have been exquisitely refined by nature (Tennessen, 2005). Unfortunately, HDPs, per se, do not represent ideal drug candidates because of drawbacks, such as reduced activity in the presence of salt, divalent cations, pH (Goldman et al., 1997; Lee et al., 1997; Minahk and Morero, 2003), plasma components, and proteases (Radzishevsky et al., 2005; Rozek et al., 2003), and because of poor pharmacokinetic (PK) issues, high systemic toxicity, and high production costs (Bradshaw, 2003; Gordon et al., 2005). Clearly, unless these concerns are properly addressed, the promise of HDPs as a new class of therapeutic agents will remain elusive.

To ameliorate the characteristic disadvantages, various synthetic peptide-mimetics that reproduce critical HDPs biophysical characteristics, such as cationicity, hydrophobicity (H), and amphipathicity in unnatural, sequence-specific oligomers, have been proposed (Patch and Barron, 2002). Generally, these HDP-mimetics are derived from a lead peptide sequence, where structural modifications have been incorporated to improve activity and/or metabolic resilience (Latham, 1999; Adessi and Soto, 2002). Examples of HDP-peptidomimetics include β peptides and peptoids, designed to mimic the overall physicochemical properties of antimicrobial peptides and shown to have characteristic secondary structures in lipid vesicles and/or in buffer. β peptides are a class of polyamides that adopt helical structures with conformational freedom greater than α peptides, because of the additional methylene unit present in the polymer backbone (Liu and DeGrado, 2001; Porter et al., 2002). Several β peptides were designed to mimic magainin and cecropin and were shown to have potent antimicrobial activity, including, however, significant activity against human erythrocytes (Liu and DeGrado, 2001). Several peptoids, oligomers of N-substituted glycines, also have stable secondary structure, despite the achirality of the polymer backbone and lack of hydrogen bond donors (Kirshenbaum et al., 1998). Certain peptoids were reported to exhibit nonhemolytic, potent antibacterial activity against both gram-positive and gram-negative bacteria (Patch and Barron, 2003). Another example is represented by facially amphiphilic arylamide polymers (Tew et al., 2002), representing another strategy to produce inexpensive synthetic polymers with broad-spectrum antibacterial activity. Regardless of these efforts and despite numerous clinical trials, no natural or modified peptide has yet obtained Food and Drug Administration approval for any (topical or systemic) medical indications (Jenssen et al., 2006).

Previous studies aimed at understanding HDPs' mechanism of action have pointed to probable target sites and stressed the significance of secondary structure. However, as HDPs contain neither a consensus sequence nor a common secondary

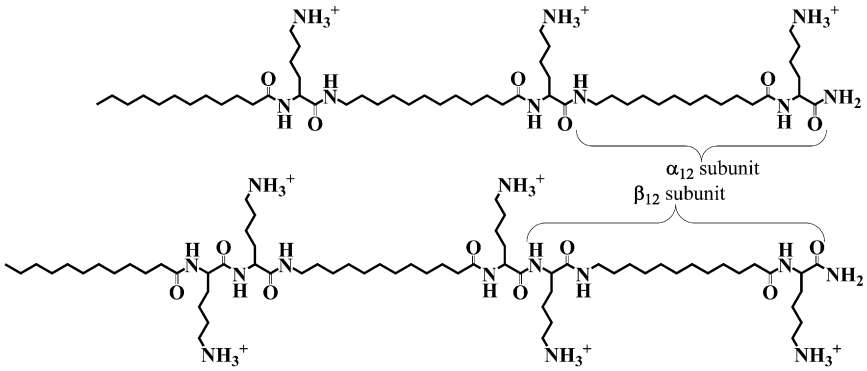

Figure 1. Molecular Structures of Typical OAKs

Parentheses point to α_{12} (aminododecanoyl-lysyl) and β_{12} (lysyl-aminododecanoyl-lysyl) subunits composing a representative α-OAK, $C_{12}K\text{-}2\alpha_{12}$ and a representative β-OAK, $C_{12}K\text{-}2\beta_{12}$ (upper and lower structures, respectively).

structure (the only common feature being the presence of both hydrophobic and positively charged amino acids), it was recently proposed that secondary structure is not required for potent antimicrobial activity (Schmitt et al., 2007; Ilker et al., 2004; Oren and Shai, 1997). This proposal was recently verified with new HDP-mimetic olygomers based on acyl-lysine (AK) subunits (referred to as α_n subunits), which were designed to inhibit formation of defined secondary structures (Radzishevsky et al., 2007a, 2007b). In a preliminary series of 16 oligoacyllysines (OAKs) composed of aminobutyryl-lysine (α_4) or aminooctanoyl-lysine (α_8) subunits, two octameric OAKs revealed potent antibacterial properties, both in vitro and in vivo. Moreover, the data suggested that OAKs design may facilitate the dissection of the relative roles of charge (Q) and H, the parameters believed to be most crucial to the activity of antimicrobial peptides.

To verify this claim, we extended the OAK library to include a total of 103 compounds intended to assess the role of composition and of sequence on antimicrobial properties. Thus, the initial group of 16 published sequences was extended to include a total of 56 OAKs based on α_4 or α_8 subunits. An additional 27 OAKs based on α_{12} subunits were investigated to further pin down the role of acyl length. Analysis of these compounds (collectively termed α-OAKs) inspired the design of 20 additional OAKs composed of β_{12} (lysyl-aminododecanoyl-lysyl) subunits designed to address the importance of sequence. The basic structure of typical α- and β-OAKs is shown in Figure 1. The overall data analysis enabled us to draw pertinent conclusions with respect to physicochemical properties required for potency and/or selectivity of OAKs.

RESULTS AND DISCUSSION

Properties of α-OAKs

An initial library of 83 α-OAKs was prepared and screened for various biophysical properties (see Table S1 in the Supplemental Data available with this article online). The library included various subseries designed to assess the importance of Q and H by systematically modifying the number of α subunits (up to 10) and the acyl length (4, 8, or 12 carbon atoms), respectively. The table lists the minimum inhibitory concentration (MIC) value of each OAK, determined against two representative bacteria (gram-negative *Escherichia coli* and gram-positive, methicillin-resistant *Staphylococcus aureus*) and the hemolytic activity determined against human red blood cells (RBC). The structure-activity relationships (SARs) that emerged from this library can be summarized as follows. Relatively few members of this library displayed the ability to inhibit bacterial growth, preferably of *E. coli*. The butyryl- and octanoyl-based series displayed activity at H ≥ 45% when Q ≥ 5, and were characteristically nonhemolytic. The dodecanoyl-based OAKs, however, displayed antibacterial activity already in the dimer $C_{12}K\text{-}\alpha_{12}$ (H = 56; Q = 2), which was also mildly hemolytic, while all longer derivatives were inactive against bacteria (MIC > 50 μM), but displayed a strong hemolytic activity. Overall, these data exposed an abnormal pattern of behavior in the dodecanoyl-based OAKs; namely, once activity had emerged, it suddenly vanished despite a further increase in Q or H or both. Moreover, it was unclear at this point why OAKs bearing very similar HQ properties would display significantly different activities. Clearly, the relatively higher H of α_{12} OAKs was responsible, but to what extent? The following experiments addressed these issues.

Organization in Solution

To probe the implication of aggregation among hydrophobic OAKs, we investigated the light scattering properties of OAKs in phosphate-buffered saline (PBS) at the range of concentrations used for bioassays. As shown in Table S1, most dodecanoyl-based OAKs were found to aggregate at low micromolar concentrations. To obtain preliminary information on the aggregate form, two representative OAKs (displaying a critical aggregate concentration [CAC] < 3 μM), composed of two and eight α_{12} subunits, were analyzed under light microscopy at two concentrations. As shown in Figure 2, the OAKs displayed distinct and concentration-independent shapes, suggesting the potential existence of at least two forms, each specific to an OAK sequence. Conversely, none of the butyryl- or octanoyl-based OAKs displayed a tendency for aggregation under these conditions, indicating that the relatively weaker hydrophobic forces of these OAKs were overcome by the positively charged lysine residues positioned relatively close to one another.

Figure 3A shows the concentration-dependent light scattering profile of a representative series of dodecanoyl-based OAKs devoid of N-terminal acyl. The data indicate that long OAKs (>4 subunits) were in the highest aggregation state, with a CAC value in the low micromolar range (estimated from the intersection with the OAK concentration axis). The shorter OAKs did not display aggregative properties, whereas the presence of an acyl at the N terminus consistently aggravated aggregation (see Table S1). These results suggested that aggregation in solution is linked to poor (or lack of) antibacterial activity of hydrophobic OAKs. Presumably, large supramolecular structures are prohibited from reaching internal targets that might be located beyond the bacterial cell wall. This notion is experimentally supported by data of

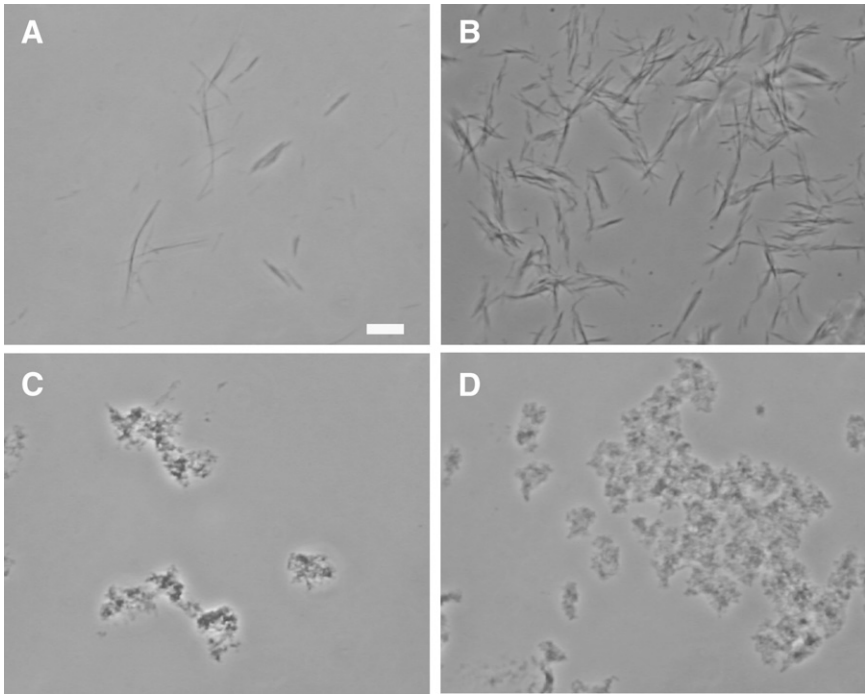

Figure 2. Light Microscope Images of OAK Aggregates

Dry samples were solubilized in PBS and examined under light microscope (phase contrast mode) 2–4 hr after preparation at room temperature. (A) C_{12}K-1α_{12} (50 μM); (B) C_{12}K-1α_{12} (500 μM); (C) C_{12}K-7α_{12} (50 μM); (D) C_{12}K-7α_{12} (500 μM). Scale bar, 10 μm.

MIC assays performed in the presence of EDTA (Figure 3B), which increases external membrane permeability. The data clearly show that formerly active compounds (those that were active in the absence of EDTA) became 4- to 8-fold more active in the presence of the cation chelator, while previously inactive OAKs revealed potent activity (i.e., activity was enhanced by up to more than 50-fold). Note that bacterial viability assessed by performing CFU counts yielded 1.46 ± 0.01 × 10^9 CFU/ml in the presence of 2 mM EDTA compared with 1.76 ± 0.05 × 10^9 CFU/ml in the absence of EDTA, indicating that EDTA alone did not significantly interfere with normal bacterial growth (Marynka et al., 2007). Thus, this assay allows the distinction between truly inactive OAKs (i.e., those that lack the HQ properties required for activity) and potentially active OAKs (i.e., the apparent inactivity of which pertains to their self-assembly in solution and, consequently, are excluded by the bacterial cell wall). The fact that all aggregated α-OAKs displayed hemolytic activity (discussed below) provides further support for this view. In contrast, antibacterial α-OAKs did not aggregate in solution.

Properties of β-OAKs

To overcome aggregation and its deleterious consequences, a heptameric OAK was used as a reference compound for further SAR investigations, as summarized in Table S2, while representative compounds are shown in Table 1. The rationale for selecting the heptamer is that this OAK reasonably represents compounds bearing HQ properties, which, a priori, should endow antibacterial activity; however, instead, they are inactive while displaying high tendencies for aggregation and hemolysis. As also shown in Figure 1, transition from α- to β-OAK (by deleting internal acyl moities) bears the structural consequence of introducing a tandem lysine (KK) motif into the oligomer sequence. Thus, deletion of three alternating acyls yielded the OAK α_{12}-3β_{12}, the H of which was significantly reduced (from 50% to 40%), while maintaining the molecular net-positive Q of the parent compound. This simultaneously led to disaggregation (CAC increased by >10-fold) and to potent, nonhemolytic antibacterial activity. Three derivatives of this particular OAK (C_{12}K-3β_{12}, C_8K-3β_{12}, and K-3β_{12}) that differentially affected H and/or Q values confirmed that high H can revert to aggregated hemolytic compounds with reduced antibacterial potency.

The remaining β-OAKs were designed to assess the effect of gradual N-terminal truncation of α_{12}-3β_{12}. Each truncation step systematically included four derivatives (NC_{12}K-nβ_{12}, C_{12}K-nβ_{12}, C_8K-nβ_{12}, and K-nβ_{12}, i.e., a total of 12 compounds where n can be 1, 2, or 3). A few β-OAKs displayed potent but unselective activity. This particularly contrasted with α-OAKs that generated preferential potency against gram-negative bacteria. The most minuscule OAK revealed by this study that displayed potent activity against both bacterial species was C_{12}K-1β_{12}, indicating that two dodecanoyl and three lysyl residues represent just about the minimal structural requirement for potent, nonselective cytotoxic properties.

In addition, a few β-OAKs seemed to hold promise for more specific activity (e.g., NC_{12}-2β_{12}). Noteworthy is the fact that the transition between these types of activities often relied on minute differences (compare, for example, C_{12}-2β_{12} and C_8-2β_{12}). The mere four carbon difference in the N-terminal acyl was responsible for drastic differences in activity profile, suggesting practically endless possibilities for future, in-depth, and fine-tuning investigations.

Finally, whereas α-OAKs were shown to maintain activity after long exposures to plasma (Radzishevsky et al., 2007b), we investigated whether the presence of the KK motif—known as a cleavage site for serine proteases, such as trypsin—might influence bioavailability. The effect of plasma over a typical β-OAK (C_{12}K-2β_{12}) was compared with a conventional antimicrobial peptide, K_4S4(1-16). The compounds were preincubated in human plasma for various time periods prior to assessing their ability to inhibit growth of *E. coli*. As shown in Figure 4, under conditions that inactivated the conventional peptide, the OAK was not affected even after longer periods of preincubation.

Relationships between HQ Values and Antibacterial Properties

The biophysical properties of the 103 compounds assessed against *E. coli* and *S. aureus* are summarized in Figure 5 to

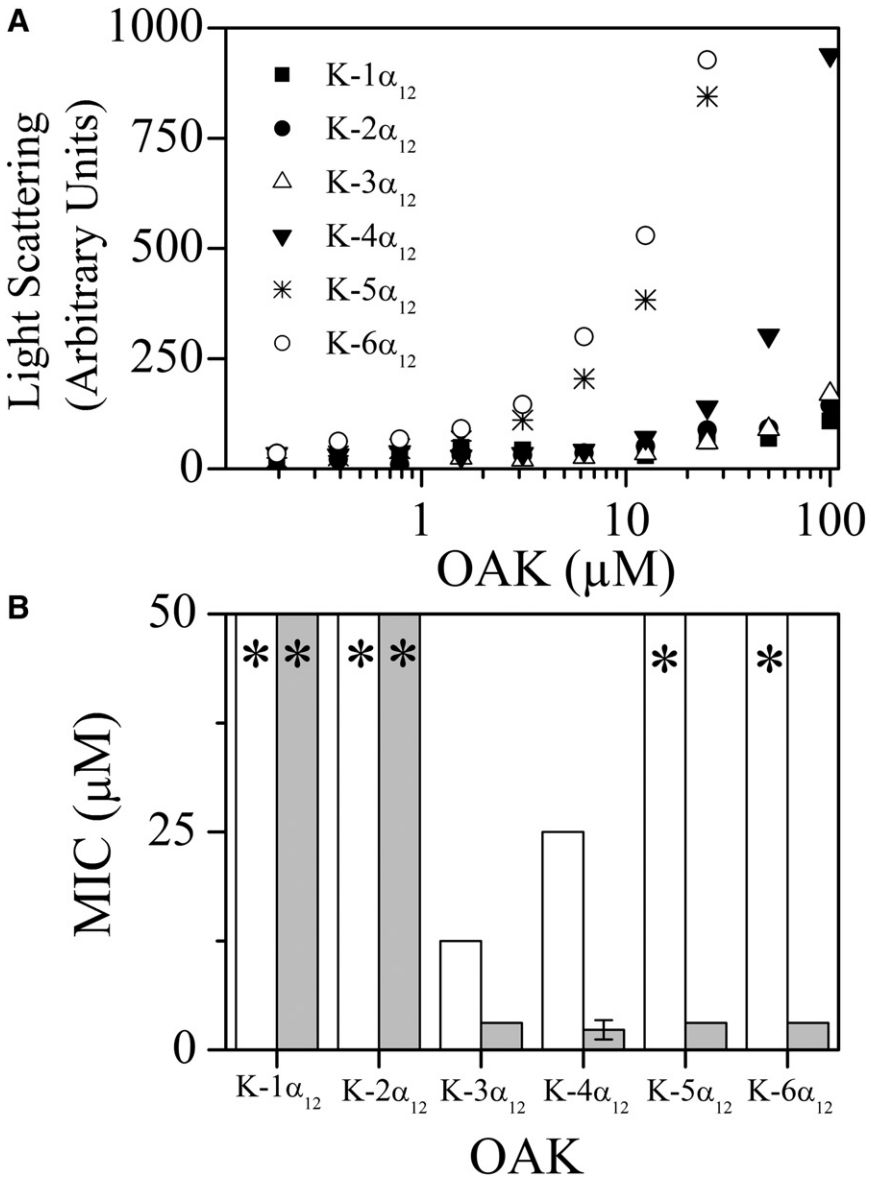

Figure 3. Relations between Self-Assembly and Antibacterial Activity

(A) The dose-dependent light scattering of a representative series of α-OAKs at the biologically relevant concentration range. CAC was evaluated by extrapolating the curve to the intercept with the x axis.

(B) The MIC against *E. coli* when assessed in the absence (white) or presence (gray) of EDTA. Asterisks indicate MIC > 50 μM. Error bars represent ±1 SD.

highlight the fact that they cover a wide range of Q (up to +11) and of H (up to 60%) values. Three major trends emerged.

First, potent antibacterial activity (MIC $\leq$ 3.1 μM) requires a relatively narrow yet specific window of HQ values, with little regard for the OAK sequence (i.e., if it is an α- or β-OAK). These values (mean and SD calculated from the H and Q values of the most active OAKs) were: H = 50 ± 2 and Q = 6.5 ± 1.9 for *E. coli*; H = 47.7 ± 7.4 and Q = 4 ± 1 for *S. aureus*. In support of this view, Figure 5B depicts the influences of acyl length and number of subunits on the MIC value of a representative series of OAKs. Thus, Figure 5B, upper panel, shows that activity of butyryl-based OAKs emerged upon attaining a certain HQ window (with maximal activity at 12 μM). The same trend was observed with octanoyl-based OAKs, but, bearing higher overall H, these OAKs attained an improved MIC value (3.1 μM). A propos, note that the longest derivative displayed a higher MIC value (reduced potency). As for the dodecanoyl-based series, only the shortest compound displayed some activity, which disappeared in longer derivatives. An overall similar trend was observed with *S. aureus* (Figure 5B, lower panel,), although OAKs of these series displayed weak anti-Staphylococcal activity at best. These data therefore suggested a reversal trend that occurred beyond the optimal HQ window. Under this assumption, we interpret these results as if the shortest dodecanoyl-based α-OAK was already beyond the optimal HQ window, as discussed below. Also, the data from Figure 5B points to the possibility that, at Q $\leq$ 5 and Q $\geq$ 6, active OAKs would display genuine specificity for gram-positive or gram-negative bacteria. Support for this view is provided by the fact that a representative OAK from each group displayed potent activity against a large panel of gram-negative bacteria (Radzishevsky et al., 2007b) and against a large panel of Staphylococcal strains (Table S3), respectively.

Second, aggregation in solution can explain discrepancies, such as why the "active HQ window" contains inactive OAKs (as depicted in Figure 3) or the fact that most hemolytic OAKs displayed a weak antibacterial activity (as discussed further below). This is not to say that all types of aggregates are necessarily inactive, especially considering that an aggregated compound can be inactive against one microorganism but active against another. An interesting example is represented by previous findings showing that short and aggregated dodecanoyl-based OAKs displayed potent antiplasmodial properties at concentrations above the CAC values (Radzishevsky et al., 2007a), supporting the notion that interactions of aggregates with eukaryotic (as opposed to prokaryotic) cells are governed by different rules, if only due to lack of a cell wall.

Third, molecular H is often dictated by the nature of the N-terminal residue. For instance, H values increased with increasing number of subunits in OAKs that lack an N-terminal acyl (e.g., OAKs 41–49), unlike in the presence of octanoyl (OAKs 25–31) or dodecanoyl (OAKs 32–40). This H stabilization enables to focus on effects specific to Q upon subunit variations.

Table 1. Biophysical Properties of Representative β_{12}-OAKs

No.	OAK Sequence[a]	Designation	Q[b]	% AcN[c]	MIC (μM)[d] *Ec*	MIC (μM)[d] *Sa*	LC_{50} (μM)[e]	CAC (μM)[f]
81	$_{NH2}$l/K/K/K/K/K/K	$7\alpha_{12}$	8	50.0	>50	>50	4.1	1.7 ± 0.5
84	$_{NH2}$l/K~~l~~/K/K~~l~~/K/K~~l~~/K/K	α_{12}-$3\beta_{12}$	8	39.5	25	>50	>100	>25
96	$_{NH2}$l-K/K-K/K	NC_{12}-$2\beta_{12}$	5	38.5	50	3.1	>100	>25
100	$_{NH2}$l/K-K/K	α_{12}-β_{12}	4	38.9	>50	>50	>100	>25

[a] ~~l~~, deleted aminododecanoyl residue; K, lysyl.
[b] Molecular charge in physiological conditions.
[c] Hydrophobicity measure, defined as the % acetonitrile eluent on a C_{18} HPLC column.
[d] Lowest OAK concentration that fully inhibited bacterial growth after 24 h culture at 37°C. *Ec*, *Escherichia coli*; *Sa*, *Staphylococcus aureus*.
[e] OAK concentration that induced 50% hemolysis (1% hematocrit) after 3 hr incubation.
[f] Critical aggregate concentration, evaluated by linear extrapolation. Values represent the mean ± SD of at least two independent experiments.

Relationships between HQ Values and Hemolytic Activity

With the exception of three or four compounds, the vast majority of the tested OAKs were revealed to belong to one of two groups: nonaggregated (CAC > 25 μM) or aggregated (CAC < 25 μM) compounds. The cut-off value of 25 μM was dictated by the method used to estimate the CAC value, which, given the OAK concentrations tested (100 μM and subsequent 2-fold dilutions), required at least three data points of light scattered above linearity (see, for example, Figure 3A). If one adopts this view, one can see a clear relationship in Figure 6 between aggregation and hemolytic activity. The fact that both occurred at high H (>45%) regardless of Q (from +2 to +11) or sequence (α- and β-OAKs) implicates hydrophobic forces in both aggregation and hemolysis. From this point of view, the exceptions that displayed a tendency for aggregation and a mild hemolytic activity are considered borderline cases, the activity profiles of which probably reflect differences in aggregate size and/or shape.

Circular dichroism (CD) measurements performed on a variety of OAKs provided further insight into organizational properties. The lower panels of Figure 6 summarize the outcome from two series of representative OAKs selected to assess the effect of acyl length and of sequence. As shown in Figure 6C, butyryl- and octanoyl-based OAKs displayed characteristic CD profiles of a random structure unlike the dodecanoyl-based OAK. Figure 6D also shows a nonrandom structure for the aggregated $7\alpha_{12}$ but not for its derivative α_{12}-$3\beta_{12}$ (resulting from deletion of three internal acyls). Increasing H through N-terminus modification increased aggregation and reverted to a nonrandom CD profile. Clearly, the CD profile obtained for aggregates are not of random structures, but rather resemble helical structures (α helix, for instance, is characterized by a positive maximum at 195 nm followed by double minima at 208 and 222 nm). These results, combined with the fact that nonrandom CD profiles were obtained only with aggregated OAKs, suggest that these profiles reflect rather supramolecular organizations. To the best of our knowledge, there are no CD studies relating to this phenomenon, but we know from experience that certain highly organized self-assemblies can display CD profiles that resemble those of classical α helix, β sheet, and others.

Thus, as previously observed with butyryl- and octanoyl-based OAKs (Radzishevsky et al., 2007b), the present CD data failed to detect a stable secondary structure in all analogous OAKs in a variety of solvent systems, including in the presence of various liposomal compositions (data not shown). With some of the dodecanoyl-based OAKs, however, the data were unambiguous in demonstrating a CD profile reminiscent to that of helical structures (Greenfield and Fasman, 1969). The strong correlation existing between aggregated OAKs and hemolytic activity provides strong support for the hypothesis underlying OAKs design (Radzishevsky et al., 2007b), implying the possibility of a link between stable folds (i.e., rigid structures) and hemolytic properties of antimicrobial peptides. Accordingly, the data indicate that incorporation of fatty acids within a peptide backbone

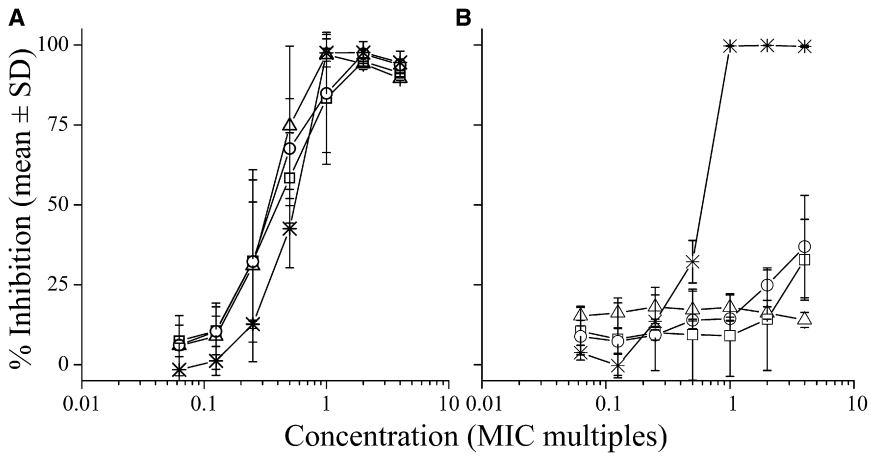

Figure 4. Inactivation by Plasma
E. coli growth inhibitory activity of $C_{12}K$-$2\beta_{12}$ (A) and a control peptide $K_4S4(1\text{-}16)$ (B) after various preincubation periods with 50% human plasma. Asterisks, control experiments (without plasma); circles, squares, and triangles indicate preincubation of 3, 6, and 18 hr, respectively. Error bars represent ± 1 SD.

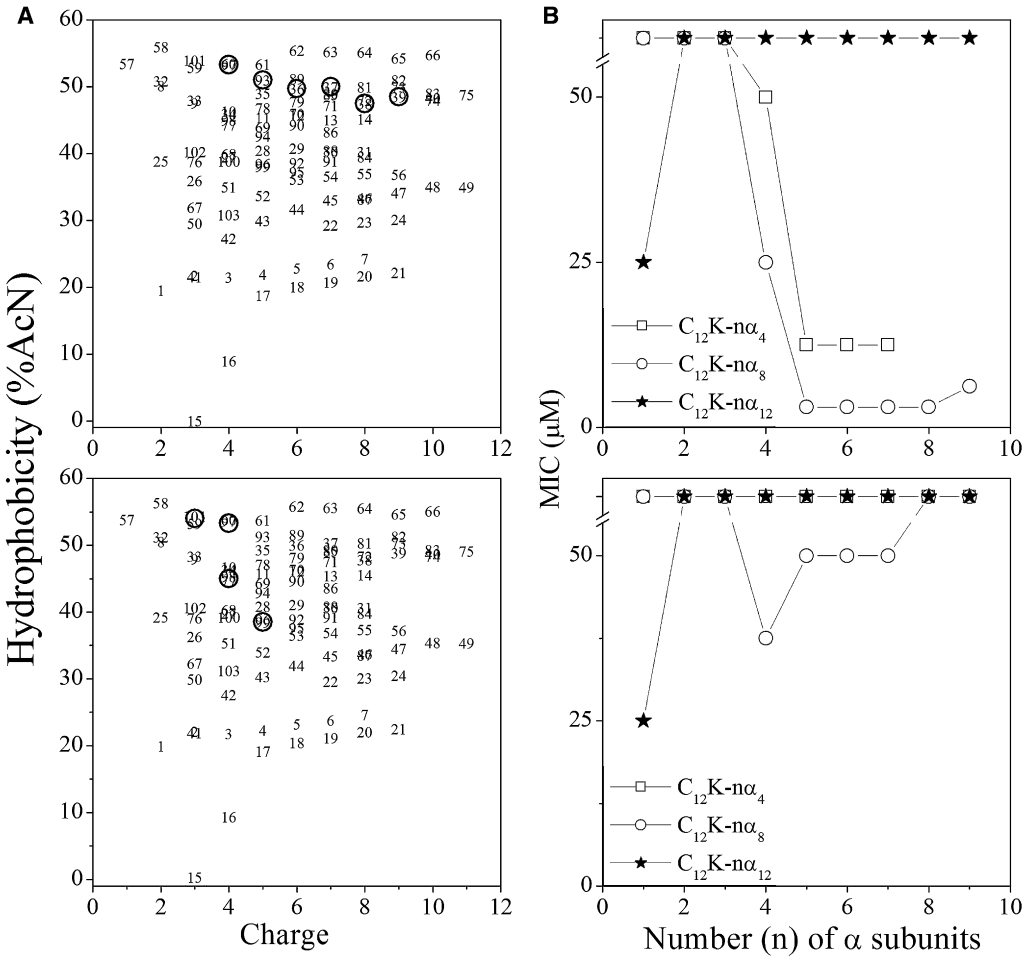

Figure 5. Relationships between HQ Properties and Antibacterial Activity

(A) The HQ map of 103 OAKs. Numbers correspond to the sequences listed in Tables S1 and S2. Circles highlight the most potent OAKs (MIC $\leq$ 3.1 μM) against *E. coli* (upper panel; OAKs 36–39, 93, and 97) and *S. aureus* (lower panel; OAKs 96–98 and 101), respectively.

(B) The effects of subunits variations on the MIC value on *E. coli* (upper panel) and *S. aureus* (lower panel), respectively.

can suppress the formation of a stable molecular fold if the acyl chain is not too long (i.e., may be longer than 8 carbon atoms, but must be shorter than 12). Conceivably, unlike short acyls, dodecanoyl residues are long enough to bend and create rigid amphipathic structures. Figure 7 depicts a drawing of such potential structures (stabilized primarily by hydrophobic interactions and eventually by hydrogen bonds between backbone amides) that can interact with RBC membrane and disrupt it—much as observed with conventional amphipathic antimicrobial peptides (Radzishevsky et al., 2005; Avrahami et al., 2001; Feder et al., 2000).

In conclusion, this study establishes that dodecanoyl-based OAKs differ from octanoyl- and butyryl-based OAKs in two respects: self-assembly and activity spectrum. Thus, the acyl chain length plays multiple and crucial roles in molecular organization and in selective activity of OAKs. This study also unraveled miniature OAKs that displayed potent and broad-spectrum activity. Some of these tiny OAKs may be difficult to use in systemic therapeutic applications due to their anticipated toxicities (e.g., high hemolytic activity), but these simple and inexpensive compounds could well be useful in other antibacterial applications, such as in cosmetics, food, or pharmaceutical technologies (Singh and Cameotra, 2004; Solans et al., 1989), and eventually in topical treatments of resilient infections.

SIGNIFICANCE

The availability of new antimicrobial compounds that are devoid of the limitations associated with current antibiotics is much desired, and the concept of providing chemically and metabolically stable, active compounds in order to achieve enhanced specificity and bioavailability has been widely acknowledged. Many designed AMPs have been presented, including ones with pseudopeptidic or peptide-mimetic structures, all touted as a novel potential new class of antibiotics. The OAK class of antimicrobial peptides is, however, quite an interesting family due to its simplicity: very few building blocks and a flexible chain arrangement presenting a novel intercalation of polar and hydrophobic residues, the sequence of which can be made to vary in quasiunlimited

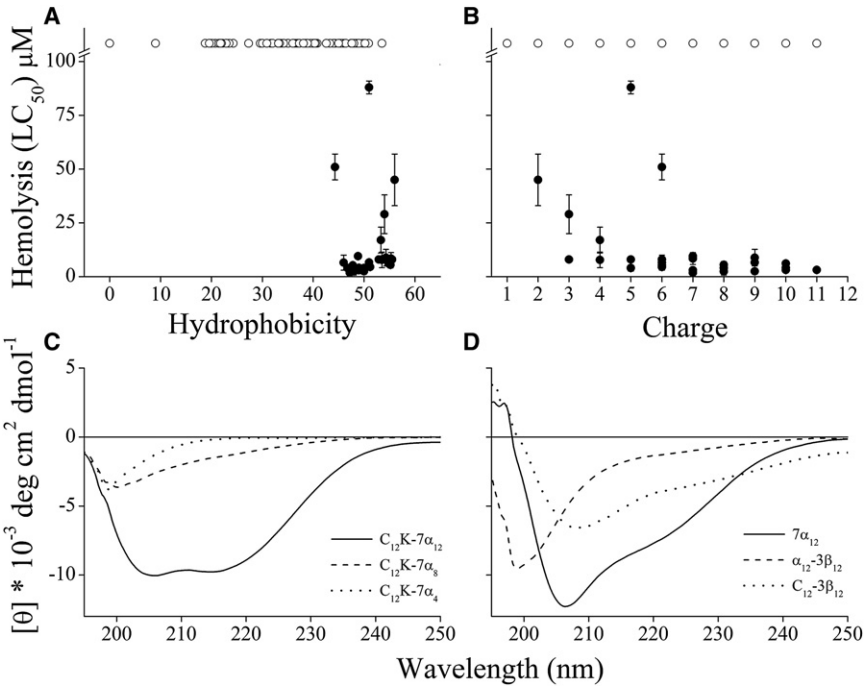

Figure 6. Hemolytic Activity and Organization in Solution

Upper panels show the hemolytic activity of 103 OAKs plotted as a function of hydrophobicity (A) or charge (B), while highlighting aggregative properties. Open circles (total of 76 OAKs) with CAC > 25 μM; closed circles (total of 27 OAKs) with CAC < 25 μM. Error bars represent ± 1 SD. Lower panels compare the circular dichroism spectra (100 μM in PBS) of three representative α-OAKs (C) and of three dodecanoyl-based α- and β-OAKs (D).

alternatives. They seem to work very well as antimicrobials, with a desirable set of characteristics (Radzishevsky et al., 2007b). Moreover, the OAK concept is likely to lead to the development of useful anti-infective agents, and could also generate valuable scientific information along the way. The simple molecules dealt with in this concept could also provide some clearer answers on specific aspects of AMP mode of action. Namely, the design of OAKs is shown to provide an efficient tool for dissecting the roles of two parameters believed to be most crucial to activity of antimicrobial peptides: hydrophobicity and charge. By analyzing a library of over 100 compounds, the data confirmed some of the claimed promises for the OAK concept. In addition, the library is shown to include a wealth of bioactive OAKs, some of which can be considered the tiniest, potent, antimicrobial peptide mimetics in the literature. Finally, the data also provide a robust basis, with practically endless possibilities, for future, in-depth, and fine-tuning investigations.

EXPERIMENTAL PROCEDURES

OAK Synthesis

The OAKs were synthesized by the solid-phase method, applying the Fmoc active ester chemistry (Fields and Noble, 1990). Fmoc-12-aminododecanoic acid, Fmoc-8-aminooctanoic acid, Fmoc-γ-aminobutyric acid, and Fmoc-amino acids were purchased from Iris Biotech GmbH (Marktredwitz, Germany). 4-Methylbenzhydrylamine resin (Novabiochem, Darmstadt, Germany) was used to obtain amidated OAKs. After synthesis, the 9-fluorenylmethoxy carbonyl was removed from the N-terminal amino acid and the OAK was cleaved from the resin with a 95/5 (v/v) mixture of trifluoroacetic acid (TFA):H_2O (20 mg of resin-bound OAK in a 1 ml mixture). The TFA was then evaporated, and the OAK was precipitated with ether followed by six cold ether washes. The crude OAKs were extracted from the resin with 30% acetonitrile in water and purified to chromatographic homogeneity in the range of >95% by reverse-phase high-pressure liquid chromatography (HPLC) and subjected to mass spectrometer analysis (Alliance-ZQ Waters). HPLC runs were performed on preparative and then on analytical C_{18} columns (Vydac) with a linear gradient of acetonitrile in water (1%/min), with both solvents containing 0.1% TFA. OAKs were stocked as lyophilized powder at −20°C. Prior to being tested, fresh solutions were

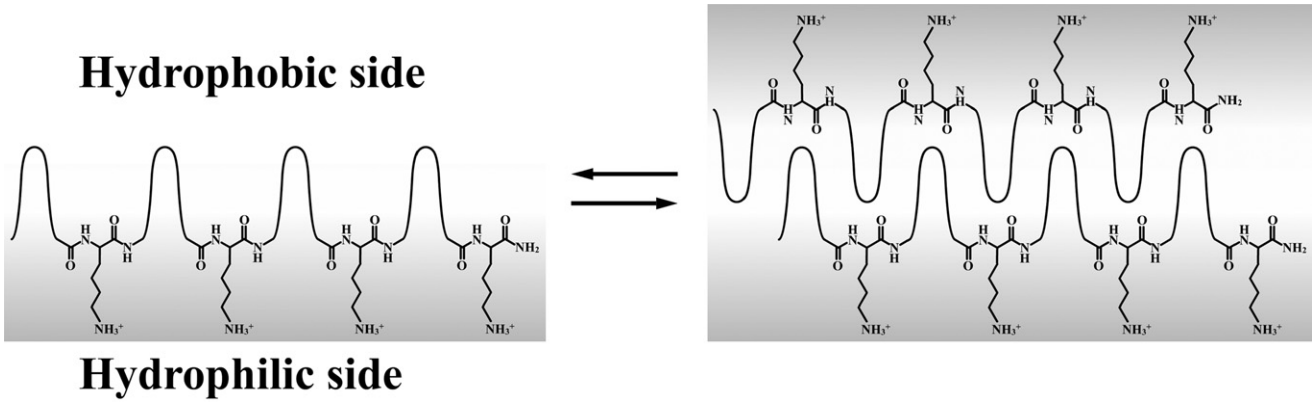

Figure 7. A Hypothetical Model for α_{12}-Oaks Organization

Shown is a representative OAK dodecanoyl-lysyl-3α_{12} in its monomeric form (left) the acyl residues of which have folded to create an amphipathic structure that can subsequently associate to form a dimer (right) or multimers (as shown in Figure 2). Such structures would be stabilized primarily by hydrophobic interactions and eventually (if packed tightly enough) by hydrogen bonds between backbone amides within each molecule in a layer and/or between molecules of adjacent layers.

prepared in water (mQ; Millipore), vortexed, sonicated, centrifuged, and then diluted in the appropriate medium.

Antibacterial Assay

MICs were determined with the microdilution assay in sterilized 96 well plates, as previously described (Radzishevsky et al., 2007b) with *E. coli* (ATCC 35218) and methicillin-resistant *S. aureus* (CI 15903) in a final volume of 200 μl as follows: bacteria were grown overnight in Luria-Bertani (LB) growth medium (10 g/l trypton, 5 g/l yeast extract, 5 g/l NaCl [pH 7.4]) and diluted 10,000-fold in growth medium. Stock solutions of the peptides were diluted 10-fold in growth medium. A 100 μl aliquot of LB containing bacteria (2–4 × 10^5 CFU/ml) was added to 100 μl of culture medium containing the test compound (0–100 μM in serial 2-fold dilutions). Inhibition of proliferation was determined by optical density measurements (620 nm) after incubation overnight at 37°C.

Enhanced Outer-Membrane Permeability Assay

The importance of self-assembly on OAKs activity against *E. coli* ATCC 35218 was explored by performing MIC experiments in the presence of 2 mM EDTA (Radzishevsky et al., 2005). Briefly, 1 M EDTA solution in water (pH 8.3) was dissolved in LB medium to 4 mM, and this solution was used for dissolving the OAKs. Growth inhibition was assessed essentially as described above.

Stability in 50% Plasma

Molecular integrity and bioavailability in plasma were essentially assessed as previously described (Radzishevsky et al., 2005). Briefly, AMP or OAK were dissolved in saline (0.9% NaCl) at an initial concentration of 64 times the MIC value, then diluted 2-fold in fresh human plasma and preincubated at 37°C. After incubation, each sample was subjected to serial 2-fold dilutions in LB medium and the MIC determined on *E. coli* ATCC 35218. Statistical data were obtained from at least two independent experiments performed in duplicates.

Light Scattering

The OAKs aggregation properties were investigated by static light scattering measurements on a Jobin-Yvon Horiba Fluorolog-3 with FluorEssence (Tanford, 1980). OAKs at an initial concentration of 100 μM were submitted to serial 2-fold dilutions down to 0.05 μM in PBS (10 mM sodium phosphate, 150 mM NaCl [pH 7.3]) at room temperature, incubated for 2 hr, and light scattering was evaluated by measuring the reflected light at an angle of 90°, holding both the excitation and the emission at 400 nm (1 nm slits). To describe the dependence of scattered signal on OAK concentration, the intensity of scattered light (mean value from at least two independent experiments) was plotted against total OAK concentrations, and a linear regression analysis was performed on the data at the concentration range close to the monomer-aggregate transition zone. Since the light scattering signal is proportional to the number of aggregated molecules and the size of the aggregate, the slope is indicative of the aggregation tendency and reveals the aggregation properties, where a slope value above unity indicates the presence of aggregative form. For aggregating OAKs, the CAC was evaluated by extrapolating the curve to the intercept with the x axis.

CD Experiments

CD spectra were recorded on a model J-810 spectropolarimeter (Jasco, Tokyo, Japan) connected to a Jasco spectra manager, with a QS Hellma quartz cell of 2 mm path length at 25°C between 190 and 250 nm at a scanning speed of 50 nm/min. The CD spectrum was scanned for OAK samples (100 μM) that were dissolved in PBS. Minor contributions of circular differential scattering were eliminated by subtracting the CD spectrum of buffer without OAK. Data values shown as mean residue molar ellipticity (degrees cm^2 $dmol^{-1}$) represent the averages of three separate recordings.

Hemolytic Assay

The OAKs potential to disrupt erythrocyte membrane was determined against human RBCs in PBS. Human blood was rinsed three times in PBS by centrifugation for 2 min at 200 × g, and resuspended in PBS at 5% hematocrite. A 50 μl suspension containing 2.5 × 10^8 RBC was added to test tubes containing 200 μl of OAKs solutions (serial 2-fold dilutions in PBS), PBS alone (for baseline values), or distilled water (for 100% hemolysis). After 3 hr incubation at 37°C under agitation, samples were centrifuged, and hemolytic activity was determined as a function of hemoglobin leakage by measuring absorbance (450 nm) of 200 μl of the supernatants.

SUPPLEMENTAL DATA

Supplemental Data include three tables and a Supplemental Reference and are available with this article online at http://www.chembiol.com/cgi/content/full/15/4/354/DC1/.

ACKNOWLEDGMENTS

This work was supported by the Israel Science Foundation (grant 387/03) and BioLineRx (grant 2006992). A.M. and I.S.R. are coinventors on patents covering the OAKs assigned to the Technion—Israel Institute of Technology and licensed to BioLineRX, a drug development company.

Received: July 26, 2007
Revised: February 21, 2008
Accepted: March 10, 2008
Published: April 18, 2008

REFERENCES

Adessi, C., and Soto, C. (2002). Converting a peptide into a drug: strategies to improve stability and bioavailability. Curr. Med. Chem. *9*, 963–978.

Avrahami, D., Oren, Z., and Shai, Y. (2001). Effect of multiple aliphatic amino acids substitutions on the structure, function, and mode of action of diastereomeric membrane active peptides. Biochemistry *40*, 12591–12603.

Bradshaw, J. (2003). Cationic antimicrobial peptides: issues for potential clinical use. BioDrugs *17*, 233–240.

Bush, K. (2004). Antibacterial drug discovery in the 21st century. Clin. Microbiol. Infect. *10* (*Suppl 4*), 10–17.

Cassell, G.H. (1997). Emergent antibiotic resistance: health risks and economic impact. FEMS Immunol. Med. Microbiol. *18*, 271–274.

Cookson, B. (2005). Clinical significance of emergence of bacterial antimicrobial resistance in the hospital environment. J. Appl. Microbiol. *99*, 989–996.

Feder, R., Dagan, A., and Mor, A. (2000). Structure-activity relationship study of antimicrobial dermaseptin S4 showing the consequences of peptide oligomerization on selective cytotoxicity. J. Biol. Chem. *275*, 4230–4238.

Fields, G.B., and Noble, R.L. (1990). Solid phase peptide synthesis utilizing 9-fluorenylmethoxycarbonyl amino acids. Int. J. Pept. Protein Res. *35*, 161–214.

Goldman, M.J., Anderson, G.M., Stolzenberg, E.D., Kari, U.P., Zasloff, M., and Wilson, J.M. (1997). Human β-defensin-1 is a salt-sensitive antibiotic in lung that is inactivated in cystic fibrosis. Cell *88*, 553–560.

Gordon, Y.J., Romanowski, E.G., and McDermott, A.M. (2005). A review of antimicrobial peptides and their therapeutic potential as anti-infective drugs. Curr. Eye Res. *30*, 505–515.

Greenfield, N., and Fasman, G.D. (1969). Computed circular dichroism spectra for the evaluation of protein conformation. Biochemistry *8*, 4108–4116.

Howard, D.H., Scott, R.D., Packard, R., and Jones, D. (2003). The global impact of drug resistance. Clin. Infect. Dis. *36*, S4–S10.

Ilker, M.F., Nusslein, K., Tew, G.N., and Coughlin, E.B. (2004). Tuning the hemolytic and antibacterial activities of amphiphilic polynorbornene derivatives. J. Am. Chem. Soc. *126*, 15870–15875.

Jenssen, H., Hamill, P., and Hancock, R.E. (2006). Peptide antimicrobial agents. Clin. Microbiol. Rev. *19*, 491–511.

Kirshenbaum, K., Barron, A.E., Goldsmith, R.A., Armand, P., Bradley, E.K., Truong, K.T., Dill, K.A., Cohen, F.E., and Zuckermann, R.N. (1998). Sequence-specific polypeptoids: a diverse family of heteropolymers with stable secondary structure. Proc. Natl. Acad. Sci. USA *95*, 4303–4308.

Latham, P.W. (1999). Therapeutic peptides revisited. Nat. Biotechnol. *17*, 755–757.

Lee, I.H., Cho, Y., and Lehrer, R.I. (1997). Effects of pH and salinity on the antimicrobial properties of clavanins. Infect. Immun. *65*, 2898–2903.

Liu, D., and DeGrado, W.F. (2001). De novo design, synthesis, and characterization of antimicrobial β-peptides. J. Am. Chem. Soc. *123*, 7553–7559.

MacKenzie, F.M., Struelens, M.J., Towner, K.J., and Gould, I.M. (2005). Report of the Consensus Conference on Antibiotic Resistance; Prevention and Control (ARPAC). Clin. Microbiol. Infect. *11*, 938–954.

Marynka, K., Rotem, S., Portnaya, I., Cogan, U., and Mor, A. (2007). In vitro discriminative antipseudomonal properties resulting from acyl substitution of N-terminal sequence of dermaseptin S4 derivatives. Chem. Biol. *14*, 75–85.

Minahk, C.J., and Morero, R.D. (2003). Inhibition of enterocin CRL35 antibiotic activity by mono- and divalent ions. Lett. Appl. Microbiol. *37*, 374–379.

Oren, Z., and Shai, Y. (1997). Selective lysis of bacteria but not mammalian cells by diastereomers of melittin: structure-function study. Biochemistry *36*, 1826–1835.

Patch, J.A., and Barron, A.E. (2002). Mimicry of bioactive peptides via non-natural, sequence-specific peptidomimetic oligomers. Curr. Opin. Chem. Biol. *6*, 872–877.

Patch, J.A., and Barron, A.E. (2003). Helical peptoid mimics of magainin-2 amide. J. Am. Chem. Soc. *125*, 12092–12093.

Paterson, D.L. (2006). The epidemiological profile of infections with multidrug-resistant *Pseudomonas aeruginosa* and *Acinetobacter* species. Clin. Infect. Dis. *43* (*Suppl 2*), S43–S48.

Porter, E.A., Weisblum, B., and Gellman, S.H. (2002). Mimicry of host-defense peptides by unnatural oligomers: antimicrobial β-peptides. J. Am. Chem. Soc. *124*, 7324–7330.

Radzishevsky, I.S., Rotem, S., Zaknoon, F., Gaidukov, L., Dagan, A., and Mor, A. (2005). Effects of acyl versus aminoacyl conjugation on the properties of antimicrobial peptides. Antimicrob. Agents Chemother. *49*, 2412–2420.

Radzishevsky, I., Krugliak, M., Ginsburg, H., and Mor, A. (2007a). Antiplasmodial activity of lauryl-lysine oligomers. Antimicrob. Agents Chemother. *51*, 1753–1759.

Radzishevsky, I.S., Rotem, S., Bourdetsky, D., Navon-Venezia, S., Carmeli, Y., and Mor, A. (2007b). Improved antimicrobial peptides based on acyl-lysine oligomers. Nat. Biotechnol. *25*, 657–659.

Rice, L.B. (2006). Antimicrobial resistance in gram-positive bacteria. Am. J. Med. *119*, S11–S19.

Roos, K.L. (2004). Emerging antimicrobial-resistant infections. Arch. Neurol. *61*, 1512–1514.

Rozek, A., Powers, J.P., Friedrich, C.L., and Hancock, R.E. (2003). Structure-based design of an indolicidin peptide analogue with increased protease stability. Biochemistry *42*, 14130–14138.

Schmitt, M.A., Weisblum, B., and Gellman, S.H. (2007). Interplay among folding, sequence, and lipophilicity in the antibacterial and hemolytic activities of α/β-peptides. J. Am. Chem. Soc. *129*, 417–428.

Singh, P., and Cameotra, S.S. (2004). Potential applications of microbial surfactants in biomedical sciences. Trends Biotechnol. *22*, 142–146.

Solans, C., Azemar, N., Infante, M.R., and Warnheim, T. (1989). Phase behavior of cationic lipoamino acid surfactant systems. In Progress in Colloid and Polymer Science, H.-G. Kilian and G. Lagaly, eds. (Berlin, Heidelberg: Springer), pp. 70–75.

Tanford, C. (1980). The Hydrophobic Effect: Formation of Micelles and Biological Membranes, Second Edition (New York: Wiley).

Tennessen, J.A. (2005). Molecular evolution of animal antimicrobial peptides: widespread moderate positive selection. J. Evol. Biol. *18*, 1387–1394.

Tew, G.N., Liu, D., Chen, B., Doerksen, R.J., Kaplan, J., Carroll, P.J., Klein, M.L., and DeGrado, W.F. (2002). De novo design of biomimetic antimicrobial polymers. Proc. Natl. Acad. Sci. USA *99*, 5110–5114.

Weber, J.T., and Courvalin, P. (2005). An emptying quiver: antimicrobial drugs and resistance. Emerg. Infect. Dis. *11*, 791–793.

White, D.G., Zhao, S., Simjee, S., Wagner, D.D., and McDermott, P.F. (2002). Antimicrobial resistance of foodborne pathogens. Microbes Infect. *4*, 405–412.

Zasloff, M. (2002). Antimicrobial peptides of multicellular organisms. Nature *415*, 389–395.

